Interfacial thermal conduction and negative temperature jump in one-dimensional lattices

Xiaodong Cao and Dahai He*

Department of Physics and Institute of Theoretical Physics and Astrophysics, Xiamen University, Xiamen 361005, Fujian, China

(Received 17 January 2015; published 25 September 2015)

We study the thermal boundary conduction in one-dimensional harmonic and ϕ^4 lattices, both of which consist of two segments coupled by a harmonic interaction. For the ballistic interfacial heat transport through the harmonic lattice, we use both theoretical calculation and molecular dynamics simulation to study the heat flux and temperature jump at the interface as to gain insights into the Kapitza resistance at the atomic scale. In the weak coupling regime, the heat current is proportional to the square of the coupling strength for the harmonic model as well as anharmonic models. Interestingly, there exists a negative temperature jump between the interfacial particles in particular parameter regimes. A nonlinear response of the boundary temperature jump to the externally applied temperature difference in the ϕ^4 lattice is observed. To understand the anomalous result, we then extend our studies to a model in which the interface is represented by a relatively small segment with gradually changing spring constants and find that the negative temperature jump still exists. Finally, we show that the local velocity distribution at the interface is so close to the Gaussian distribution that the existence or absence of a local equilibrium state is unable to be determined by numerics in this way.

DOI: 10.1103/PhysRevE.92.032135 PACS number(s): 05.70.Ln, 44.10.+i, 05.90.+m

I. INTRODUCTION

Since its observation between liquid helium and a metal [1], thermal boundary resistance, namely, Kapitza resistance, has been extensively studied theoretically and experimentally [2]. With the rapid development of modern electronic technology, there has been much interest in understanding the fundamental nature of thermal boundary conductance since it has been a significant obstacle in designing micro- and nanoscale electronic chips. Two phenomenological models, the acoustic mismatch model [3] and diffuse mismatch model [2], have been proposed to study the mechanism of the thermal boundary conductance. However, because they neglect atomic details at the interface, they both offer limited accuracy, particularly for nanoscale interfacial resistance [4]. To understand the mechanism of thermal boundary conductance at the atomic level, many studies have been done in one-dimensional lattices via different methods [4–6]. Most of the previous studies focus on the effect of the interface on the steady-state heat flux and little attention has been paid to the temperature jump between the interface from the atomic viewpoint.

On the other hand, heat conduction in low-dimensional dynamical systems has become the subject of a large number of theoretical and experimental studies in recent years [7–9]. An exact approach to interacting Hamiltonian systems is so far unavailable except for harmonic crystals. A meaningful definition of local temperature depends on the local thermal equilibrium and it is difficult to give a microscopic derivation of the condition in general [10]. With the usual definition of local temperature, i.e., the mean local kinetic energy, the temperature profile may show some unexpected features, such as the temperature oscillations in the steady state of alternate mass hard particle gas [11], in the Fermi-Pasta-Ulam chain [12], and in harmonic chain with alternating mass [13].

In the present study, we study the heat flux and temperature jump at the interface to gain insights into the Kapitza resistance at the atomic scale via theoretical calculations and molecular dynamics simulations. We find that there exists a negative temperature jump between the interfacial particles in particular parameter regimes. A nonlinear response of the boundary temperature jump to the externally applied temperature difference in the ϕ^4 lattice is observed. Note that although the *interface* between two segments is not well defined in one-dimensional Hamiltonian systems, our studies can give some insights into the thermal boundary resistance in real systems.

The paper is organized as follows. In Sec. II we define the model and give the methods for theoretical calculations and molecular dynamics simulations. In Sec. III we demonstrate the existence of negative temperature jump in both the harmonic and ϕ^4 model. Finally, we give a brief summary and discussion in Sec. IV.

II. MODEL AND METHODS

We study the nonequilibrium steady state of a one-dimensional chain consisting of two coupled lattices,

$$H = H_L + H_R + \tfrac{1}{2}k_c(x_{N/2} - x_{N/2+1})^2. \tag{1}$$

The Hamiltonians for the left and right segments are given by

$$H_L = \sum_{i=1}^{N/2}\left(\frac{p_i^2}{2m} + \frac{f_L}{2}x_i^2 + \frac{\lambda_L}{4}x_i^4\right) + \frac{k_L}{2}\sum_{i=0}^{N/2-1}(x_i - x_{i+1})^2,$$

$$H_R = \sum_{i=N/2+1}^{N}\left(\frac{p_i^2}{2m} + \frac{f_R}{2}x_i^2 + \frac{\lambda_R}{4}x_i^4\right) + \frac{k_R}{2}\sum_{i=N/2+1}^{N}(x_i - x_{i+1})^2, \tag{2}$$

where x_i denotes the displacement of the ith particle from its equilibrium position. Fixed boundary conditions are taken, i.e., $x_0 = x_{N+1} = 0$. The particles 1 and N at the two ends are connected to the heat baths at temperature T_L and T_R, respectively. The heat baths are modeled by the Langevin

*dhe@xmu.edu.cn

equations corresponding to Ohmic baths; i.e., the self-energy of the baths are $\Sigma(\omega) = i\gamma\omega$ [8].

When $\lambda_L = \lambda_R = 0$, the on-site potential and interparticle interaction are all quadratic. In the classical limitation, the steady heat current from left to right reservoir can be given by the Langevin equations and Green's function (LEGF) method [8,14],

$$J = \frac{k_B(T_L - T_R)}{\pi}\int_{-\infty}^{\infty} d\omega \mathrm{Tr}[G_S^+(\omega)\Gamma_L(\omega)G_S^-(\omega)\Gamma_R(\omega)], \tag{3}$$

with

$$G_S^{\pm}(\omega) = \frac{1}{[-\omega^2 M_S + K_S - \Sigma_L^{\pm}(\omega) - \Sigma_R^{\pm}(\omega)]}, \tag{4}$$

$$\Gamma_{L,R}(\omega) = \mathrm{Im}(\Sigma_{L,R}^{+}(\omega)), \tag{5}$$

where M_S and K_S denote the mass matrix and force constant matrix of the system. Note that $G_S^{\pm}, \Sigma_{L,R}^{\pm}$ are all $N \times N$ matrices for one-dimensional systems. The only nonzero elements of $\Sigma_{L,R}^{\pm}$ are respectively $[\Sigma_L^{\pm}]_{1,1} = \Sigma = i\gamma\omega$ and $[\Sigma_L^{\pm}]_{N,N} = \Sigma = i\gamma\omega$. γ is the coupling strength of the first and Nth particle to the left and right reservoirs, respectively. The velocity-velocity correlation and position-velocity correlation are

$$K = \langle \dot{\tilde{X}}_S \dot{\tilde{X}}_S^T \rangle = \frac{k_B T_L}{\pi}\int_{-\infty}^{\infty} d\omega\omega G_S^+(\omega)\Gamma_L(\omega)G_S^-(\omega) + \frac{k_B T_R}{\pi}\int_{-\infty}^{\infty} d\omega\omega G_S^+(\omega)\Gamma_R(\omega)G_S^-(\omega), \tag{6}$$

$$C = \langle \tilde{X}_S \dot{\tilde{X}}_S^T \rangle = \frac{ik_B T_L}{\pi}\int_{-\infty}^{\infty} d\omega G_S^+(\omega)\Gamma_L(\omega)G_S^-(\omega) + \frac{ik_B T_R}{\pi}\int_{-\infty}^{\infty} d\omega G_S^+(\omega)\Gamma_R(\omega)G_S^-(\omega). \tag{7}$$

The correlation function K can be used to define local energy density, which can in turn be used to define the local temperature, i.e.,

$$T_i = mK_{i,i}, \tag{8}$$

and C gives the local heat current density [15–18]. We integrate Eqs. (3) and (6) numerically to obtain the steady-state heat current and local temperature, for which the rectangular method is used [19]. We also verify that the local current, obtained by integrating Eq. (7) numerically, is the same along the chain, which is one of the properties in the steady state.

When $\lambda_L, \lambda_R \neq 0$, we apply the nonequilibrium molecular dynamics simulation (NEMD) to the system, for which the Langevin heat baths are used at the two ends of the chain. The equations of motion are given by

$$m\ddot{x}_i = -\frac{\partial H}{\partial x_i} - \gamma_i \dot{x}_i + \eta_i, \tag{9}$$

where $\gamma_i = \gamma(\delta_{1,i} + \delta_{N,i})$ and $\eta_i = \eta_L\delta_{1,i} + \eta_R\delta_{N,i}$. The noise terms $\eta_{L,R}$ denote a Gaussian white noise with zero mean and variance of $2\gamma k_B T_{L,R}$. The local heat flux is given by $j = \langle F(x_{i+1} - x_i)v_{i+1}\rangle$, where $F(x) = -V'(x)$ and the notion $\langle\cdots\rangle$ denotes a steady-state average. The equations of motion [Eq. (9)] are integrated by using a second-order stochastic Runge-Kutta algorithm [20]. At steady states, the numerically computed local heat flux is always constant along the chain, and the local temperature is defined as $T_i = m\langle \dot{x}_i^2 \rangle$. To compute the boundary temperature jump, i.e., $\Delta T_b = T_{N/2} - T_{N/2+1}$, the relaxation and average time must be both long enough. In what follows we set $m = 1, k_B = 1$, and $\gamma = 1$.

III. RESULTS AND DISCUSSION

For many devices of several segments, interfacial coupling is pretty weak, which indicates that k_c is far less than k_L and k_R in our model. So it is desirable to study the thermal transport through atomic chains in the weak coupling regime. It has been shown that [21] the heat current is proportional to the square of the coupling strength in one-dimensional weakly coupled chain with the Morse on-site potential by a phenomenological analysis. Is this square-law relation between heat current and coupling strength still valid in the weak coupling limit when the anharmonic on-site potential is absent? As shown in Fig. 1, we plot the heat current as a function of the coupling strength in the weak coupling limit by integrating Eq. (3) numerically. It turns out that the square law relation is still valid when the anharmonicity is absent. Furthermore, the square law relation still holds when the system consists of symmetrical or asymmetrical segments with or without an on-site potential.

Figure 2 shows the steady-state heat current and the boundary temperature jump as a function of the coupling strength k_c. The reason to carry out both theoretical calculation and NEMD simulation is to verify that the results we obtained are from physical reasons rather than numerical uncertainty. Note that the temperature jump between the $N/2$-th particle and the $(N/2+1)$-th particle is sensitive to heat fluctuation when k_c approaches to k_R, which requires high-precision simulations. By inspecting the figure, we can see that theoretical

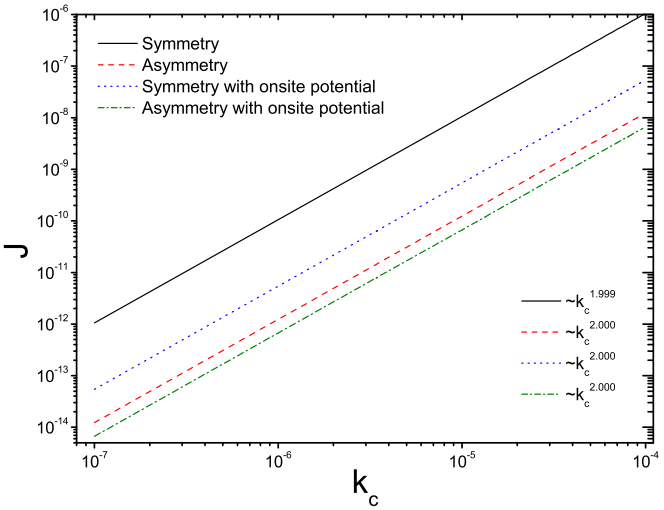

FIG. 1. (Color online) Heat flux as a function of interfacial coupling k_c via the LEGF approach as k_c approaches to zero. Symmetry: $k_L = k_R = 1, f_L = f_R = 0$; asymmetry: $k_L = 1, k_R = 2, f_L = f_R = 0$; symmetry with on-site potential: $k_L = 1, k_R = 1, f_L = f_R = 2$; and asymmetry with on-site potential: $k_L = 1, k_R = 2, f_L = f_R = 2$. For all cases, we set $T_L = 2, T_R = 1$ and $N = 64$.

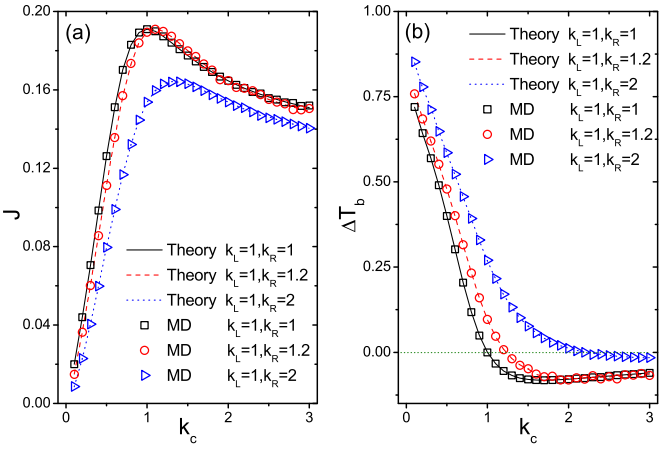

FIG. 2. (Color online) The heat flux (a) and temperature jump between the $N/2$-th and $(N/2+1)$-th particles (b) as a function of k_c via both the LEGF approach and MD simulations. Here $f_L = f_R = 0, T_L = 2, T_R = 1, \lambda_L = \lambda_R = 0$, and $N = 64$. In panel (b), the horizontal dotted line is drawn as a reference line for $\Delta T_b = 0$.

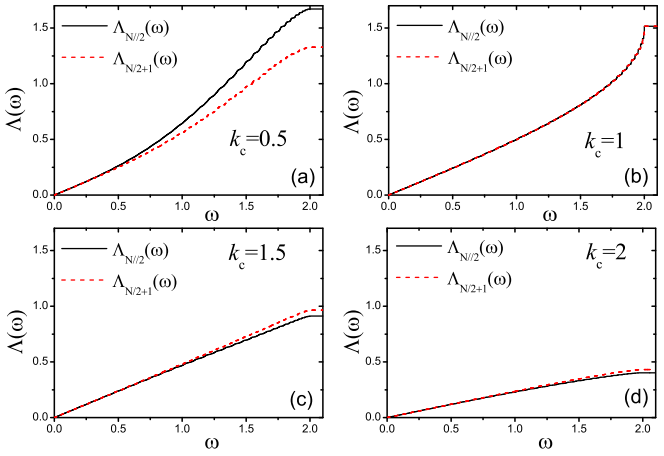

FIG. 3. (Color online) The contribution of normal modes to local temperature at the interface for (a) $k_c = 0.5$, (b) $k_c = 1$, (c) $k_c = 1.5$, and (d) $k_c = 2$, respectively. Here $k_L = k_R = 1$, $f_L = f_R = 0$, $\lambda_L = \lambda_R = 0$, $T_L = 2, T_R = 1$, and $N = 64$.

calculations and MD simulations agree well with each other. The heat current increases at first, arrives at a maximum value, and then slightly decreases with the increase of k_c. As depicted in Fig. 2, the maximum heat current occurs at $k_c = 2k_Lk_R/(k_L + k_R)$, which agrees with the result obtained in Ref. [5] by the scattering boundary method. Furthermore, both theoretical calculations and MD simulations indicate that there is a negative boundary temperature jump, i.e., $\Delta T_b < 0$, when k_c approaches to k_R. The word *negative* is in contrast with normal heat conduction where the direction of the heat flow is from hot to cold regions. In fact, similar negative temperature jumps occurs in several systems, for example, the temperature jump between the second and third particles and between the $(N-2)$-th and $(N-1)$-th particles in the uniform harmonic chain [7] coupled with reservoirs, and the temperature oscillations in the steady state of hard particle gas [11], the Fermi-Pasta-Ulam chain [12], and the harmonic chain [13] with alternating mass. To understand the negative temperature jump at the interface, we need to inspect the concept of the local temperature further. The local temperature of the ith particle can be written as $T_i = \Lambda_i(\omega_{\max})$, with

$$\Lambda_i(\omega) = 2\int_0^{\omega} d\omega' \left(\frac{k_B T_L}{\pi} \omega' G_S^+(\omega') \Gamma_L(\omega') G_S^-(\omega') + \frac{k_B T_R}{\pi} \omega' G_S^+(\omega') \Gamma_R(\omega') G_S^-(\omega') \right), \tag{10}$$

and $\omega_{\max}$ is the top boundary of the phonon spectra. The kinetic energy of a particle gets contributions from all the modes, and the net result depends on the distribution of energy in the different modes. As shown in Fig. 3, we plot the contribution of normal modes to the local temperature for the $(N/2)$-th and $(N/2+1)$-th particles by integrating Eq. (10) numerically. As we can see, *equipartition* among phonon modes, i.e., each normal mode shares the same average kinetic energy, is not satisfied for $k_c = 0.5$ and $k_c = 1$ shown by the nonlinear behaviors of $\Lambda_i(\omega)(i = N/2, N/2+1)$ in the high-frequencies region. Surprisingly, for the case of $k_c = 1.5$, $\Lambda_i(\omega)$ exhibit almost linear behavior with increasing ω, indicating that the contributions to the local temperature from possible phonon modes are closely equivalent. By comparing them with $k_c = 0.5$, we can see that the high-frequency normal modes are suppressed more dramatically than the low-frequency normal modes for $k_c = 1.5$ and $k_c = 2$, and the turning of $\Lambda_{N/2}$ and $\Lambda_{N/2+1}$ in the high-frequencies region indicates the negative temperature jump between the $N/2$-th and $(N/2+1)$-th particles.

It would be interesting to see if the negative temperature jump is an artificial effect due to the integrability of the harmonic system. Thus we conduct similar studies in the ϕ^4 lattice, which has additional nonlinear on-site potential on each site in comparison with the harmonic system. We plot the boundary temperature jump ΔT_b as a function of the external temperature difference $\Delta T = T_L - T_R$ and some typical temperature profiles in Fig. 4. One can see that the boundary temperature jump is proportional to ΔT for $k_c < 1$ and proportional to $(-\Delta T)$ for $k_c > 1$ when ΔT is small, which are typical linear-response behaviors shown in harmonic models. With the increasing of ΔT, the linear behavior of ΔT_b no longer holds for the ϕ^4 lattice. Note that negative temperature jump occurs when $k_c \geqslant 1.3$ and the absolute value of ΔT_b nonlinearly increases as ΔT increases.

So far our discussions is based on the model consisting of two segments with a single harmonic coupling, which inevitably leads to the argument that the origin of negative temperature jump comes from the ill-defined interface of the two-segment model with a sharp discontinuity of the interfacial coupling. In what follows we propose an extended model to show that it is not the case. Actually, in a practical consideration, the interface may be a junction which is small compared with the two sublattices. So we divide our system into three regions, say, two sublattices and a junction. The particle number of the junction is small compared with the two sublattices. The spring constant of the intermediate segment varies smoothly, which is done by setting the spring constants of the intermediate junction by $k_i = \exp[-(i - N/2)^2/50] + 1$, where i represents the index of particles. The NEMD

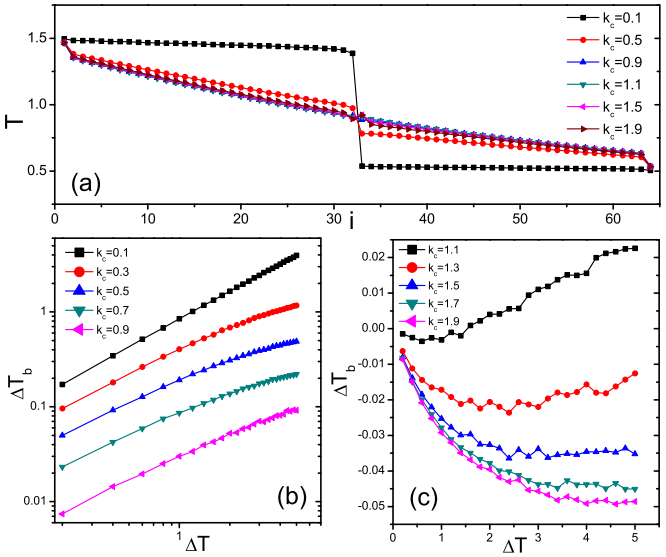

FIG. 4. (Color online) (a) Temperature profile in the ϕ^4 lattice for $k_c = 0.1$, 0.5, 0.9, 1.1, 1.5, and 1.9, respectively. (b) ΔT_b as a function of ΔT for $k_c < 1$. (c) ΔT_b as a function of ΔT for $k_c > 1$. The lines in panels (a), (b), and (c) are drawn to guide the eyes. Here we set $T_L = T_R + \Delta T$, $T_R = 0.5$, $\lambda_L = \lambda_R = 1$, $k_L = k_R = 1$, and $N = 64$.

simulation results of harmonic and ϕ^4 lattices are presented in Figs. 5 and 6, respectively. As we can see, negative temperature gradient still exists for both harmonic and ϕ^4 lattices within the interfacial segment.

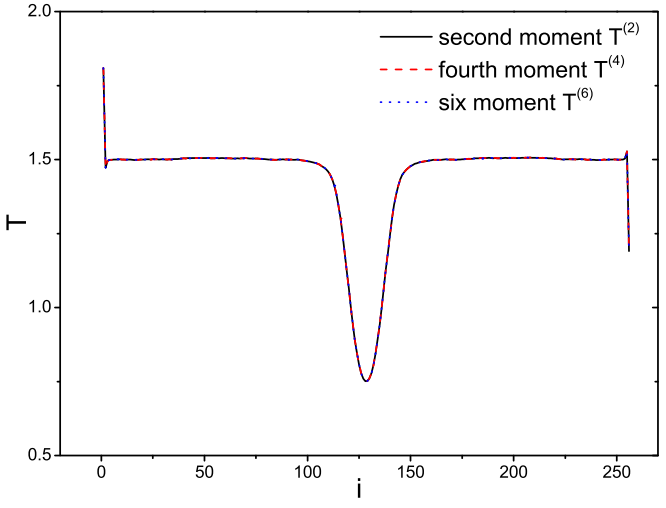

FIG. 5. (Color online) The temperature profile of the harmonic chain with an interfacial junction, whose spring constants are smoothly varied. The distribution of spring constants for the whole system is given as follows: $k_i = k_L = 1$ for $1 \leqslant i \leqslant 7N/16$; $k_i = \exp[-(i - N/2)^2/50] + 1$ for $7N/16 < i \leqslant 9N/16$; and $k_i = k_R = 1$ for $9N/16 < i \leqslant (N - 1)$, where i is the index of particle number and $N = 256$. The first three even moments of velocity are given by $T_i^{(2)} = m\langle \dot{x}_i^2 \rangle$ for the second moment, $T_i^{(4)} = m(\langle \dot{x}_i^4 \rangle/3)^{1/2}$ for the fourth moment and $T_i^{(6)} = m(\langle \dot{x}_i^6 \rangle/15)^{1/3}$ for the sixth moment, respectively. Here $T_L = 2, T_R = 1$, and $N = 256$.

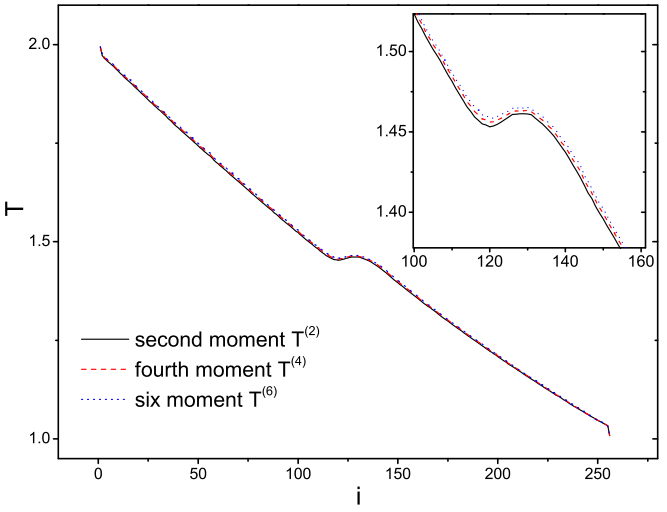

FIG. 6. (Color online) The temperature profile of the ϕ^4 lattice with an interfacial junction, whose spring constants are smoothly varied. The distribution of the spring constants in the interfacial junction is the same as that for Fig. 5. Here $\lambda_L = \lambda_R = 1, T_L = 2$, $T_R = 1$, and $N = 256$.

As mentioned above, a meaningful local temperature can be defined only in systems exhibiting local thermal equilibrium. And we know that, if the system can exhibit local thermal equilibrium, the local distribution should be Gaussian and all even moments can be obtained based on the second moment. We can then use $T_i^{(2)} = m\langle \dot{x}_i^2 \rangle$, $T_i^{(4)} = m(\langle \dot{x}_i^4 \rangle/3)^{1/2}$, and $T_i^{(6)} = m(\langle \dot{x}_i^6 \rangle/15)^{1/3}$ to define local temperature equivalently, so we carry out NEMD simulation for both the harmonic and ϕ^4 lattice and plot the local temperature defined by the first three even moments of velocity, namely, the second, fourth, and sixth moments in Figs. 5 and 6. To our surprise, the local temperatures defined by $T^{(2)}$, $T^{(4)}$, and $T^{(6)}$ at the boundary particles agree well with each other. The deviation at the interface is not significant in comparison with the inside segments. The result indicates the local distribution is at least very close to the Gaussian, which cannot be well distinguished by numerics and should be examined with more careful theoretical studies of local distribution in the future.

IV. SUMMARY

We have studied interfacial thermal conductance in one-dimensional inhomogeneous systems by using both theoretical calculations and MD simulations. In the weak coupling limit, theoretical calculations show that the heat current is proportional to the square of the coupling strength in the absence of anharmonicity. A negative temperature jump between the interfacial particles occurs in both the harmonic and ϕ^4 lattices. To understand the counterintuitive observation, we have investigated the contribution of normal modes to the local temperature at the interface. It is shown that the high-frequency modes make dominant contributions when the coupling strength is small; however, the contribution of each mode is almost equivalent when the coupling strength is strong. We have confirmed that the occurrence of the

negative temperature jump is not trivially artificial due to the integrability of the system or the sharp discontinuity of the interfacial coupling by extending the system to a model consisting of two sublattices and an intermediate junction for both the harmonic and ϕ^4 lattices.

One should re-examine the notion of temperature to understand the anomalous negative temperature jump, which seemingly indicates that heat flows against a local temperature gradient in a small scale. On the one hand, from the viewpoint of traditional thermodynamics, local temperature should be defined in a cell, which should be macroscopically infinitesimal but contain enough microscopic degrees of freedom. Such kind of cell is, strictly speaking, not well defined for our microscopic model due to the large atomic-scale fluctuations and the word *local* defined for a single oscillator loses its inherent meaning. On the other hand, we stress that the traditional definition of local temperature with respect to the kinetic energy of an oscillator is still in the framework of equilibrium thermodynamics. The anomalous phenomenon may partly comes from the definition as used here, which lacks a complete description of the nonequilibrium steady state. A new definition of *nonequilibrium temperature* might be taken into consideration on this count [22,23], especially when one take notice of the temperature profile for the middle region of the intermediate junction, which is anomalously smaller than T_R, as shown in Fig. 5. However, whether the concept of (local) temperature can be extrapolated beyond local equilibrium or should be modified in the nonequilibrium systems is still an open question.

ACKNOWLEDGMENTS

The authors thank Y. Zhang, J. Wang, and H. Zhao for helpful discussioins and Xiamen Supercomputer Center for use of its computing facilities. This work was financially supported by the National Nature Science Foundation of China (Grants No. 11047185, No. 11105112, and No. 11335006).

[1] W. J. Abbe, Nuovo Cimento **56**, 187 (1968).
[2] E. T. Swartz and R. O. Pohl, Rev. Mod. Phys. **61**, 605 (1989).
[3] W. Little, Can. J. Phys. **37**, 334 (1959).
[4] M. E. Lumpkin, W. M. Saslow, and W. M. Visscher, Phys. Rev. B **17**, 4295 (1978).
[5] L. Zhang, P. Keblinski, J.-S. Wang, and B. Li, Phys. Rev. B **83**, 064303 (2011).
[6] D. He, S. Buyukdagli, and B. Hu, Phys. Rev. B **80**, 104302 (2009).
[7] S. Lepri, R. Livi, and A. Politi, Phys. Rep. **377**, 1 (2003).
[8] A. Dhar, Adv. Phys. **57**, 457 (2008).
[9] J.-S. Wang, J. Wang, and J. T. Lü, Eur. J. Phys. B **62**, 381 (2008).
[10] F. Bonetto, J. Lebowitz, and L. Rey-Bellet, in *Mathematical Physics 2000* (Imperial College Press, London, 2000), p. 128.
[11] P. L. Garrido, P. I. Hurtado, and B. Nadrowski, Phys. Rev. Lett. **86**, 5486 (2001).
[12] T. Mai, A. Dhar, and O. Narayan, Phys. Rev. Lett. **98**, 184301 (2007).
[13] V. Kannan, A. Dhar, and J. L. Lebowitz, Phys. Rev. E **85**, 041118 (2012).
[14] A. Dhar and D. Roy, J. Stat. Phys. **125**, 805 (2006).
[15] A. Dhar and B. S. Shastry, Phys. Rev. B **67**, 195405 (2003).
[16] A. Dhar, Phys. Rev. Lett. **86**, 5882 (2001).
[17] R. J. Rubin and W. L. Greer, J. Math. Phys. **12**, 1686 (1971).
[18] A. J. O'Connor and J. L. Lebowitz, J. Math. Phys. **15**, 692 (1973).
[19] W. H. Press, S. A. Teukolsky, W. T. Vetterling, and B. P. Flannery, *Numerical Recipes: The Art of Scientific Computing*, 3rd ed. (Cambridge University Press, New York, 2007).
[20] R. L. Honeycutt, Phys. Rev. A **45**, 600 (1992).
[21] B. Hu, D. He, L. Yang, and Y. Zhang, Phys. Rev. E **74**, 060101 (2006).
[22] G. P. Morriss and L. Rondoni, Phys. Rev. E **59**, R5 (1999).
[23] J. Casas-Vzquez and D. Jou, Rep. Prog. Phys. **66**, 1937 (2003).